



This article appeared in a journal published by Elsevier. The attached copy is furnished to the author for internal non-commercial research and education use, including for instruction at the authors institution and sharing with colleagues.

Other uses, including reproduction and distribution, or selling or licensing copies, or posting to personal, institutional or third party websites are prohibited.

In most cases authors are permitted to post their version of the article (e.g. in Word or Tex form) to their personal website or institutional repository. Authors requiring further information regarding Elsevier's archiving and manuscript policies are encouraged to visit:

<http://www.elsevier.com/copyright>



Water in nanoconfined and biological environments (Plenary Talk, Ngai-Ruocco 2009 IDMRCS Conf.)[☆]

H.E. Stanley^{a,*}, S.V. Buldyrev^b, P. Kumar^a, F. Mallamace^c, M.G. Mazza^a, K. Stokely^a, L. Xu^d, G. Franzese^e

^a Center for Polymer Studies and Department of Physics, Boston University, Boston, MA 02215 USA

^b Department of Physics, Yeshiva University, 500 West 185th Street, New York, NY 10033 USA

^c Dipartimento di Fisica, Univ. Messina, Vill. S. Agata, C.P. 55, I-98166 Messina, Italy

^d World Premier International (WPI) Research Center, Advanced Institute for Materials Research, Tohoku University, Sendai 980-8577, Japan

^e Departament de Física Fonamental, Univ. de Barcelona, Diagonal 647, Barcelona 08028, Spain

ARTICLE INFO

Available online 27 November 2010

Keywords:
Water;
Polyamorphism;
Critical point

ABSTRACT

We discuss some recent progress in understanding the anomalous behavior of liquid water, by combining information provided by recent experiments and simulations on water in bulk, nanoconfined, and biological environments. We interpret evidence from recent experiments designed to test the hypothesis that liquid water may display “polymorphism” in that it can exist in two different phases – and discuss recent work on water’s transport anomalies as well as the unusual behavior of water in biological environments. Finally, we will discuss how the general concept of liquid polymorphism may prove useful in understanding anomalies in other liquids, such as silicon, silica, and carbon, as well as metallic glasses which have in common that they are characterized by two characteristic length scales in their interactions.

© 2010 Elsevier B.V. All rights reserved.

1. Water: a complex liquid

Water is vital for life [1]. Not surprisingly, then, water though seemingly simple in its chemical formula, is a very complex liquid. In particular, its phase diagram is rich and complex, with more than sixteen crystalline phases [2], and two or more glasses [3–5]. The liquid state also displays complex behavior, such as the density maximum for 1 atm at 4 °C. The volume fluctuations $(\delta V)^2$, entropy fluctuations $(\delta S)^2$, and cross-fluctuations between volume and entropy $\delta V \delta S$, proportional to the magnitude of isothermal compressibility K_T , isobaric specific heat C_p , and isobaric thermal expansivity α_p , respectively, show anomalous increases in magnitude upon cooling [6]. Further, data on all three quantities are consistent with a possible “apparent divergence” for 1 atm at -45 °C [6], a phenomenon that has attracted many scientists and which hints at interesting phase behavior in the deeply supercooled region.

Microscopically, liquid water’s anomalous behavior is understood as resulting from the tendency of neighboring molecules to form hydrogen bonds (H-bonds) upon cooling, with a decrease of local potential energy, decrease of local entropy, and increase of local volume due to the formation of “open” local structures of bonded molecules. Different models include these H-bond features, but depending on the assumptions and approximations of each model, different conclusions are obtained for the low-T phase behavior. The

relevant region of the liquid state cannot readily be probed experimentally, so a great deal of ingenuity has been used to obtain the results we have.

2. Four scenarios for understanding low-temperature water

Due to the difficulty of obtaining experimental evidence, theoretical and numerical analyses are useful. Four different scenarios for the pressure–temperature (P – T) phase diagram have been proposed:

- (I) The *stability limit* (SL) scenario [7] hypothesizes that the superheated liquid–gas spinodal at negative pressure re-enters the positive P region below the temperature $T_H(P)$ of homogeneous nucleation of the crystal ice. In this view, the liquid state is delimited by a single continuous locus, $P_s(T)$, bounding the superheated, stretched and supercooled states. There is no reference to the phase into which the liquid transforms when $P \rightarrow P_s(T)$. As the spinodal is approached, K_T , C_p , and $|\alpha_p| \rightarrow \infty$. A thermodynamic consequence of the SL scenario is that the intersection of the retracing spinodal with the liquid–vapor coexistence line must be a critical point [3]. The presence of such a critical point in the liquid–vapor transition, although possible, is not confirmed by any experiment. This fact poses a serious challenge to the SL scenario.
- (II) The *liquid–liquid critical point* (LLCP) scenario [8] hypothesizes a first-order phase transition line between two liquids – a low density liquid (LDL), and a high density liquid (HDL) – which terminates at a liquid–liquid critical point C' . HDL is a dense

[☆] Dedicated to the memory of Professor Victoria Buch.

* Corresponding author.

E-mail address: hes@bu.edu (H.E. Stanley).

liquid with a highly disordered structure, whereas LDL has a lower density and locally tetrahedral order. The experimentally observable high density amorphous (HDA) and low density amorphous (LDA) solids correspond, in this scenario, to a structurally arrested state of HDL and LDL respectively [9,10]. Starting from C' , the locus of maxima of the correlation length ξ (the Widom line) projects into the one-phase region [11,12]. Asymptotically close to the critical point, response functions can be expressed in terms of ξ , hence, these too will show maxima, e.g., as a function of T upon isobaric cooling. These maxima will diverge upon approaching C' . However along paths that miss the critical point, these functions will display maxima, a phenomenon discussed in the context of water by Sciortino et al. [13]. Furthermore, for $P > P_{C'}$, the pressure of C' , the response functions will diverge by approaching the spinodal converging to C' . Specific models suggest [8,14] that $P_{C'} > 0$, but the possibility $P_{C'} < 0$ has also been proposed [15,16].

- (III) The *singularity-free* (SF) scenario [17] hypothesizes that the low- T anticorrelation between volume and entropy is sufficient to cause the response functions to increase upon cooling and display maxima at non-zero T , without reference to any singular behavior [18,19]. Specifically, Sastry et al. [17] consider the temperature of maximum density (TMD) line, where the density has a maximum as a function of temperature, and prove a general thermodynamic theorem establishing the proportionality between the slope of the TMD, $(\partial P/\partial T)_{\text{TMD}}$, and the temperature derivative of K_T . Thus, since the TMD has negative slope in water, i. e. $(\partial P/\partial T)_{\text{TMD}} < 0$, it follows that K_T must increase upon cooling, whether there exists a singularity or not.
- (IV) The *critical-point free* (CPF) scenario [20] hypothesizes an order-disorder transition, with possibly a weakly first-order transition character, separating two liquid phases and extending to $P < 0$ down to the superheated limit of stability of liquid water. This scenario effectively predicts a continuous locus of stability limit spanning the superheated, stretched [21] and supercooled state, because the spinodal associated with the first-order transition will intersect the liquid-gas spinodal at negative pressure. No critical point is present in this scenario.

These four scenarios predict fundamentally different behavior, though each has been rationalized as a consequence of the same microscopic interaction: the H bond [22–24]. A question that naturally arises is whether the macroscopic thermodynamic descriptions are in fact connected in some way. Previous works have attempted to uncover relations between several of the scenarios, for example between (I) and (II) [14,25] or (II) and (III) [26,27]. Recently, Stokely et al. [28] offered a relation linking all four scenarios showing that (a) all four can be included in one general scheme, and (b) the balance between the energies of two components of the H bond interaction determines which scenario is valid (Fig. 1). Moreover, they argue that current values for these energies support the LLCP scenario.

3. Selected experimental results

Current experiments on this problem are of two sorts. The first is a set of experiments on *bulk* water inspired by Mishima that involves probing the No Man's Land by studying the metastable extensions of the melting lines of the various high-pressure polymorphs of ice: ice III, ice V, ice IV, and ice XII [29,30]. Two of these lines clearly display “kinks.” Since the slope of any melting line is the difference of the volume change divided by the entropy change of the two phases that coexist at that line, if there is a change in slope there must be a change in these quantities. Since there is no change in the crystal part, there must be a change in the liquid part. This means the liquid must undergo a jump in either its volume or its entropy or both. That is the definition of a first-order phase transition.

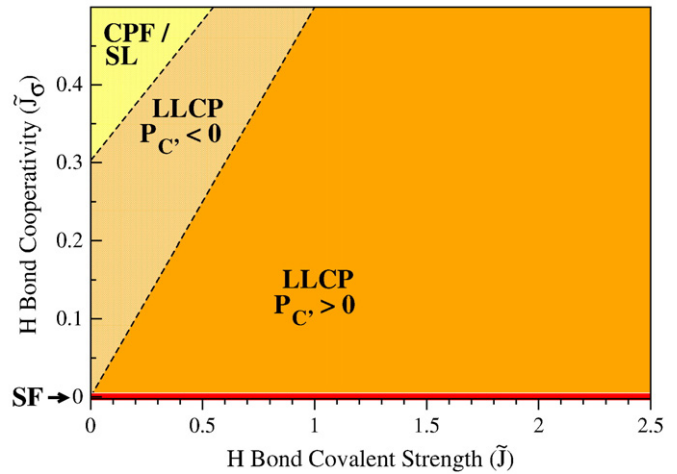


Fig. 1. Possible scenarios for water for different values of H bond energies \tilde{J} of the covalent (or directional) component, and \tilde{J}_σ of the cooperative (or many-body) component, obtained from MF calculations [28]. (i) If $\tilde{J}_\sigma = 0$ (red line along X-axis), the singularity free (SF) scenario is realized, independent of \tilde{J} . (ii) For large enough \tilde{J}_σ , water would possess a first-order liquid–liquid phase transition line terminating at the liquid–gas spinodal—the critical point free (CPF) scenario; the liquid spinodal would retrace at negative pressure, as in the stability limit (SL) scenario (yellow region in top left). (iii) For other combinations of \tilde{J} and \tilde{J}_σ , water would be described by the liquid–liquid critical point (LLCP) scenario. For larger \tilde{J}_σ , the LLCP is at negative pressure (ochre region between dashed lines). For smaller \tilde{J}_σ , the LLCP is at positive pressure (orange region in bottom right). Dashed lines separating the three different regions correspond to MF results of the microscopic cell model. The P - T phase diagram evolves continuously as \tilde{J} and \tilde{J}_σ change.

A second set of experiments is being carried out on *confined* water in the MIT group of Chen and the Messina group of Mallamace, which have stimulated many of our recent calculations. Mallamace, Chen, and their collaborators succeeded in locating the Widom line by finding a clearcut maximum in the coefficient of thermal expansion, at $T_W \approx 225$ K [31], which remarkably is the same temperature as the specific heat maximum [32]. Also, private discussions with Jacob Klein reveal a possible reason for why confined water does not freeze at -38 C, the bulk homogeneous nucleation temperature: Klein et al. [33] noted that confined water behaves differently than typical liquids in that water does not experience the huge increase in viscosity characteristic of other strongly confined liquids. They interpret this experimental finding as arising from the fact that strong confinement hampers the formation of a hydrogen bonded network, and we know from classic work of Linus Pauling that without the extensive hydrogen bonded network, water's freezing temperature will be depressed by more than 100 degrees. Thus confinement reduces the extent of the hydrogen bonded network and hence lowers the freezing temperature, but appears to leave the key tetrahedral local geometry unchanged.

4. Theoretical predictions and experimental tests of the liquid–liquid critical point and singularity free scenarios

Using Monte Carlo simulations and mean field calculations, a cell model of water proposed by Franzese et al. [12,34–36] can reproduce all four scenarios that have been discussed for water. Kumar et al. [37–39] found that both the LLCP and SF scenarios exhibit a dynamic crossover at the temperature of the maximum isobaric specific heat C_p , $T(C_p^{\text{max}})$, which decreases for increasing P . They interpret the dynamic crossover as a consequence of a local breaking and reorientation of the bonds for the formation of new and more tetrahedrally oriented bonds. Above $T(C_p^{\text{max}})$, when T decreases, the number of hydrogen bonds increases, giving rise to an increasing activation energy E_A and to a non-Arrhenius dynamics. As T decreases,

entropy must decrease. A major contributor to entropy is the orientational disorder, that is a function of p_B , the probability of forming a hydrogen bond, as described by the mean field expression for the entropy change ΔS with orientation. They found that, as T decreases, p_B increases. They found that the rate of increase has a maximum at $T(C_p^{\text{max}})$, and as T continues to decrease this rate drops rapidly to zero – meaning that for $T < T(C_p^{\text{max}})$, the local order rapidly becomes temperature-independent and the activation energy E_A also becomes approximately temperature-independent. Corresponding to this fact the dynamics becomes approximately Arrhenius.

They found that the relaxation time at the crossover temperature T_A is approximately independent of the pressure (isochronic crossover) consistent with their calculations of an almost constant number of bonds at $T(C_p^{\text{max}})$. They found also that E_A and T_A decrease upon increasing P in both LLC and SF scenarios. Instead, the P dependence of the quantity $E_A/(k_B T_A)$ has a different behavior in the two scenarios, although the difference is about 1%. For the LLC scenario it increases as $P \rightarrow P_c$, while it is approximately constant in the SF scenario. They interpret this difference as a consequence of the larger increase of the rate of change of p_B in the LLC scenario, where p_B diverges at finite T_c , compared to the SF scenario, where p_B can possibly diverge only at $T=0$. Experiments can detect local changes of water structure from HDL-like to LDL-like, (e.g., [40]). Hence, it is possible to test the

predictions on the dynamic consequences of this local change. Franzese et al. [41] found that three of the four predictions made by Kumar et al. in [37,38] are verified in experiments. Indeed, Chen and collaborators verified that the crossover is isochronic, and that E_A and T_A decrease upon increasing P . The fourth prediction about the behavior of $E_A/(k_B T_A)$, discriminating between the two possible scenarios, cannot be verified within the precision of the experiment [42].

5. The Widom line emanating from every critical point into the one-phase region

By definition, in a first order phase transitions, thermodynamic state functions such as density ρ and enthalpy H discontinuously change as we cool the system along a path crossing the equilibrium coexistence line [Fig. 2(a), path β]. In a real experiment, this discontinuous change may not occur at the coexistence line since a substance can remain in a supercooled metastable phase until a limit of stability (a spinodal) is reached [43] [Fig. 2(b), path β]. If the system is cooled isobarically along a path above the liquid-gas critical pressure P_c [Fig. 2(b), path α], the state functions continuously change from the values characteristic of a high temperature phase (gas) to those characteristic of a low temperature phase (liquid). The

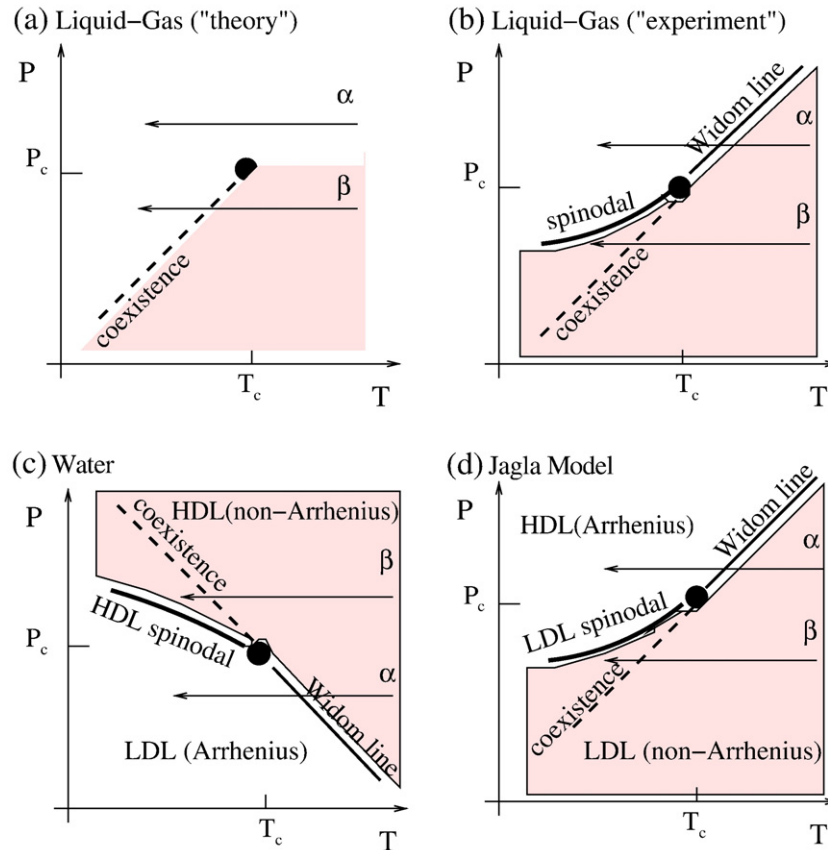


Fig. 2. (a) Schematic phase diagram for the critical region associated with a liquid–gas critical point. Shown are the two features displaying mathematical singularities, the critical point (closed circles) and the liquid–gas coexistence (bold dashed curve). (b) Same as (a) with the addition of the gas–liquid spinodal and the Widom line. Along the Widom line, thermodynamic response functions have extrema in their T dependence. The path α denotes a path along which the Widom line is crossed. Path β denotes a path meeting the coexistence line. (c) A hypothetical phase diagram for water of possible relevance to the recent neutron scattering experiments by Chen et al. [60,61] on confined water. The liquid–liquid coexistence, which has a negative sloped coexistence line, generates a Widom line which extends below the critical point, suggesting that water may exhibit a dynamic crossover (non-Arrhenius-to-Arrhenius) transition for $P < P_c$ (path α), while no dynamic changes will occur above the critical point (path β). (d) A sketch of the P – T phase diagram for the two-scale Jagla model. For the Jagla potential, as well as for the shouldered potentials [109–112], the liquid–liquid phase transition line has a positive slope. Upon cooling at constant pressure above the critical point (path α), the liquid changes from a low density state (characterized by a non-glassy Arrhenius dynamics) to a high density state (characterized by glassy Arrhenius dynamics with much larger activation energy) as the path crosses the Widom line. Upon cooling at constant pressure below the critical point (path β), the liquid remains in the LDL phase as long as path β does not cross the LDL spinodal line. Thus one does not expect any change in the dynamic behavior along the path β , except upon approaching to glass transition where one can expect the non-Arrhenius behavior characterized by the Vogel–Fulcher–Tamman (VFT) fit.

thermodynamic response functions which are the derivatives of the state functions with respect to temperature [e.g., isobaric heat capacity $C_p \equiv (\partial H / \partial T)_p$] have maxima at temperatures denoted by $T_{\max}(P)$. Remarkably these maxima are still prominent far above the critical pressure [11,12,32,44,45], and the values of the response functions at $T_{\max}(P)$ (e.g., C_p^{\max}) diverge as the critical point is approached. The lines of the maxima for different response functions asymptotically approach one another as the critical point is approached, since all response functions become expressible in terms of the correlation length. This asymptotic line is sometimes called the Widom line, and is often regarded as an extension of the coexistence line into the “one-phase regime” [11].

Water's anomalies have been hypothesized to be related to the existence of a line of a first order liquid–liquid phase transition terminating at a liquid–liquid critical point [3,8,29,36,43,46], located below the homogeneous nucleation line in the deep supercooled region of the phase diagram – sometimes called the “no-man's land” because it is difficult to make direct measurements on the bulk liquid phase [29]. In supercooled water, the liquid–liquid coexistence line and the Widom line have negative slopes. Thus, if the system is cooled at constant pressure P_0 , computer simulations suggest that for $P_0 < P_c$ [Fig. 2(c), path α] experimentally-measured quantities will change dramatically but continuously in the vicinity of the Widom line (with huge fluctuations as measured by, e.g., C_p) from those resembling the high density liquid (HDL) to those resembling the low density liquid (LDL). For $P_0 > P_c$ [Fig. 2(c), path β], experimentally-measured quantities will change discontinuously if the coexistence line is actually seen. However, the coexistence line can be difficult to detect in a pure system due to metastability, and changes will occur only when the spinodal is approached where the HDL phase is no longer stable. The changes in behavior may include not only static quantities like response functions but also dynamic quantities like diffusivity [32,44,45]. See in particular the very recent work of Ruocco et al. [47,48].

In the case of water, a significant change in dynamical properties has been suggested to take place in deeply supercooled states of bulk [3,49] and confined water [50–52]. Unlike other network forming materials, water behaves as a non-Arrhenius liquid in the experimentally accessible window [3]. Based on analogies with other network forming liquids and with the thermodynamic properties of the amorphous forms of water, it has been suggested that, at ambient pressure, liquid water should show a dynamic crossover from non-Arrhenius behavior at high T to Arrhenius behavior at low T [11,37,53]. Using Adam–Gibbs theory [54], the dynamic crossover in water was related to the C_p^{\max} line [11,37,49,55]. Also, a dynamic crossover has been associated with the liquid–liquid phase transition in simulations of silicon and silica [56–59]. Recently a dynamic crossover in confined water was studied experimentally [60–62] since nucleation can be avoided in confined geometries.

6. Appearance of a fractional Stokes–Einstein relation in water and a structural interpretation of its onset

The Stokes–Einstein (SE) relation has long been regarded as one of the hallmarks of transport in liquids. It predicts that the self-diffusion constant D is proportional to $(\tau/T)^{-1}$, where τ is the structural relaxation time and T the temperature. Xu et al. [63] recently presented their experimental results on water confined in MCM-41-S nanotubes. They measured the self-diffusion D by nuclear magnetic resonance (NMR), and they measured the translational relaxation time τ by using incoherent, quasi-elastic neutron scattering (QENS) [64,65]. Thus, the SE relation,

$$D \sim (\tau/T)^{-1}, \quad (1)$$

can be tested. Their data [Fig. 3(a)] confirmed Eq. (1) at high temperatures, but showed that, upon cooling below a crossover

temperature $T_\times \approx 290$ K, the SE relation (1) gave way to a “fractional SE relation” [65–69],

$$D \sim (\tau/T)^{-\zeta}, \quad (2)$$

with $\zeta \approx 0.62$.

They interpreted the microscopic origin of this crossover by analyzing the OH stretch region of the FTIR spectrum over a wide T range from 350 K down to 200 K. Simultaneous with the onset of fractional SE behavior, they found that water begins to develop a local structure like that of low-density amorphous solid H₂O. These data lead to an interpretation that the fractional SE relation in water arises from a specific change in local water structure. To further test this interpretation, they performed computer simulations of two molecular models, and their simulation results supported their experimental observations.

As a first step to obtain a structural interpretation this fractional SE behavior, they turn to measurements of the infrared spectrum [64,65,70–72]. For water this spectrum can be split into two contributions, one resembling the spectrum of HDA solid H₂O and the other resembling the spectrum of LDA solid H₂O. They interpret these two contributions as corresponding to water molecules with more HDA-like local structure, or more LDA-like local structure, respectively [73,74]. They show in Fig. 3(b) the relative populations of molecules with locally LDA-like structure and molecules with locally HDA-like structure calculated by decomposition of the infrared spectra. With decreasing T , the LDA-like population increases, while the HDA-like population decreases. The fractional SE crossover temperature T_\times appears to roughly coincide with the onset of the increase of the population of molecules with LDA-like local structure (and a corresponding decrease of the population of the molecules with HDA-like local structure), consistent with the possibility that the changes in intramolecular vibrational properties may be connected to the onset of fractional SE behavior.

To more clearly see the change in the relative populations of molecules with LDA-like local structure (and, correspondingly, with HDA-like local structure), they calculate the derivatives of the relative populations with respect to temperature [Fig. 3(c)]. The derivatives of the relative populations become noticeably non-zero at the same value of the crossover temperature, $T_\times \approx 290$ K. In contrast, we find that the maximal rate of change of the vibrational spectrum occurs at a much lower temperature, $T_{\max} \approx 245$ K, approaching the Widom temperature 225 K for bulk water [49].

Concerning simulations: since experiments on bulk water at $T < 250$ K are impractical due to crystallization, Yamada et al. perform constant- T and constant-density molecular dynamics simulations of $N = 512$ water molecules interacting with the TIP5P potential [91] at a fixed density $\rho = 1$ g/cm³. Additionally, direct access to the molecular coordinates makes it possible to connect the changes in D to changes in the local molecular structure.

The relaxation time τ is defined as the time when the coherent intermediate scattering function decays by a factor of e for the wave vector q of the first peak of the static structure factor. Unlike the relaxation time of the incoherent intermediate scattering function, the coherent relaxation time closely tracks the T dependence of the viscosity (viscosity is used in the original formulation of the SE relation). The diffusion coefficient is computed from the root mean square displacement of the oxygens as a function of temperature. Analogous to the experimental results in Fig. 3(a), we simulated D for TIP5P water for as a function of τ/T . We found that below $T_\times \approx 320$ K the SE relation crosses over to a fractional SE relation [92] of Eq. (2) with $\zeta = 0.77$, similar to the exponent observed in SPCE water [92].

We observed a gradual increase in LDA-like local structures, and a decrease in HDA-like local structure. The derivatives of the relative populations of the LDA-like and the HDA-like molecules with respect to temperature show that the change does not have a sharp onset at

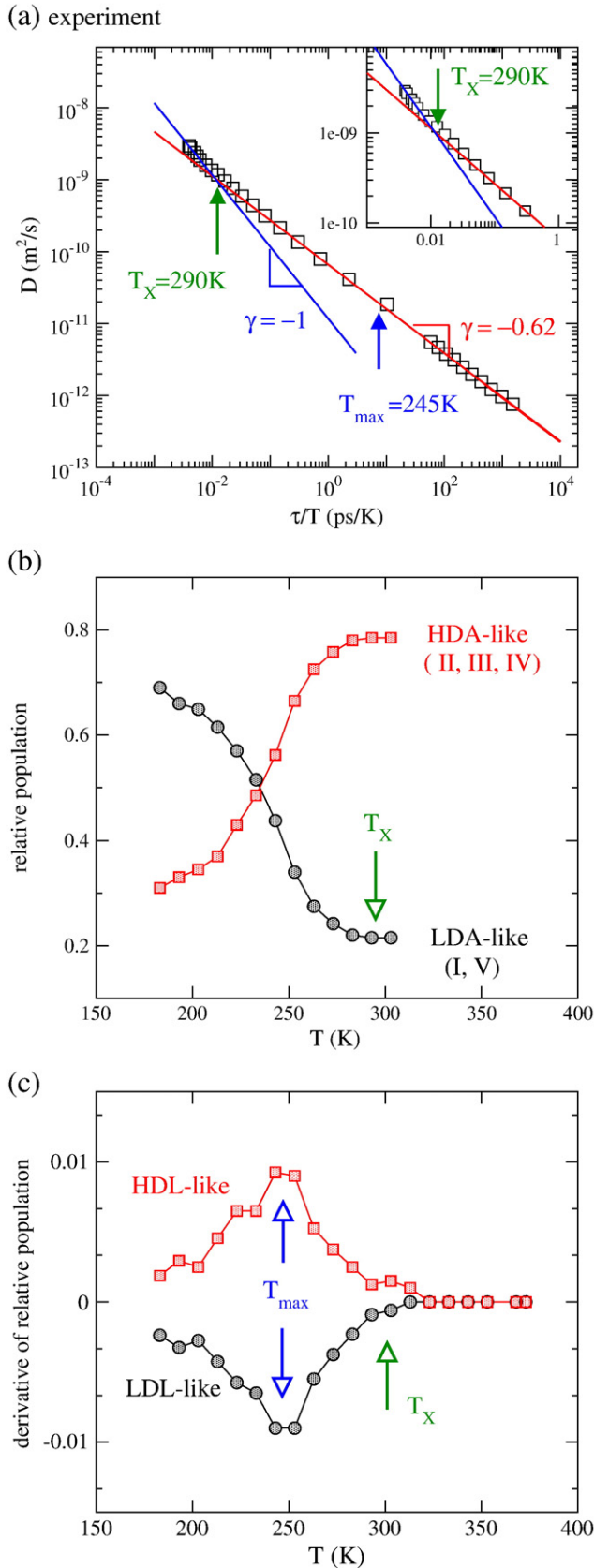


Fig. 3. Experimental results for water at $P=1$ bar. (a) Parametric relation of D as a function of τ/T . The onset of the fractional SE relation around $T_x \approx 290$ K is indicated by the change of slope from $\zeta = 1$ to $\zeta = 0.62$, while $T_{max} \approx 245$ K is determined from panel (c). (b) The relative population of different species of water molecules in experiment. (c) The derivative of the relative population with respect to temperature for LDA-like and HDA-like species.

$T_x \approx 320$ K. For each species (LDA-like and HDA-like), the maximum change defines a temperature $T_{max} \approx 255$ K for the structural evolution [63,93]. Like our experimental results, $T_x > T_{max}$ for TIP5P, indicating that the change to fractional SE behavior can be connected with the emergence of more highly structured regions of the liquid, rather than the maximal rate of change.

Both our experimental findings and our simulation results are consistent with the possibility that in water the fractional SE relation (2) sets in near the temperature where the relative populations of molecules with LDA-like and HDA-like local structures start to rapidly change. A structural origin for the failure of the SE relation can be understood by recognizing that the SE relation defines an effective hydrodynamic radius. The different species have different hydrodynamic radii, so when their relative populations changes, the classical SE relation (based on the assumption of the fixed hydrodynamic radius) breaks down. Moreover, a connection between the local structure of water and its dynamics is expected [92,94,95]; molecules with a locally tetrahedral geometry are more “sluggish” than less well-networked molecules. This effect also occurs in solutions, where a failure of the scaling between diffusion and relaxation has been interpreted in terms of changes in the local network structure [96,97]. For these reasons, our structure-based interpretation for the failure of the SE relation is particular to water. An explanation for the failure of the SE relation for liquids in general must involve understanding how the intermittency of the molecular motion couples to diffusion and relaxation mechanisms near the glass transition. For the majority of liquids, the breakdown of SE occurs within 30% of the glass transition temperature, while for water it occurs at almost twice the glass transition temperature. For the case of water, the emergence of such intermittency of the dynamics is inseparable from water’s unusual thermodynamics and corresponding changes in the fluid structure.

7. To what degree are experiments on confined water relevant to understanding bulk water?

Since these experiments examine water confined to cylindrical pores of ≈ 2 nm diameter, it is natural to question whether the experimental findings might be instructive for understanding bulk water at low T . There are many reasons to be concerned about the degree to which experiments on confined water are relevant to “real water”. For example, the fact that confinement suppresses the melting temperature by about 100 K shows that at least one property of confined water differs drastically from the corresponding property of bulk water. This issue is not completely resolved, as there exist currently arguments that are not in agreement.

On the one hand, recent experiments suggest the answer is “no”. The similarities between bulk and water confined in MCM-41-S have been recently challenged by a neutron diffraction work [75]. This has clearly shown that the cross correlation term between water and silica not only is not negligible but it is also temperature dependent, as it reflects the balance between water–water and water silica surface interactions (see Fig. 2 of [74]). In addition, coupling neutron diffraction data with a Monte Carlo simulation, it has been shown that confined water cannot be considered as a homogeneous fluid filling the available pore volume. The microscopic structure of water changes depending on the distance from the pore wall and on temperature. Concerning the interaction between water and silica, see also the recent careful work of Findenege et al. [76].

There are two reasons that suggest the answer may be “yes”: (i) computer simulations of confined water on a hydrophilic surface [77] show that hydrophilic silica-confined water has similar behavior as bulk water, indicating that the hydrophilic surfaces do not have serious effects on the properties of water, except for significantly lowering the freezing temperature and stabilizing the liquid phase which allows the study of supercooled region made impossible in bulk water due to crystallization; (ii) the presence of hysteresis in a

temperature cycle (upon cooling/heating) is a signature of an interaction between water and silica. However, for the MCM-41-S confined system, only negligible hysteresis was observed by means of X-ray scattering and calorimetric experiment [78,79].

A different category of potential concern arises from the fact that the comparison of simulation/theory results with experiments thus far is limited to MCM41-S, to three biological systems (lysozyme, DNA, and RNA) and to cement. In any case, it is plausible that the disturbance brought by the confining matrix to water can be considered negligible for larger pore sizes, but the experimental fact is that water freezes for pore sizes larger than about 2 nm.

Recently Gallo et al. [80], building on their wealth of experience studying confined liquids [81–90] have accurately tested the degree to which the experiments on MCM-41 confined water are in agreement with simulations in confined geometries.

8. The tetrahedral entropy and tetrahedral specific heat reflecting space-time correlations in the tetrahedral order parameter

Very recently Kumar et al. [93] introduced the space-dependent correlation function $C_Q(r)$ and time-dependent autocorrelation function $C_Q(t)$ of the local tetrahedral order parameter $Q \equiv Q(r, t)$ [98]. Using computer simulations of 512 waterlike particles interacting through the TIP5P potential, they investigated $C_Q(r)$ in a broad region of the phase diagram. They found that at low temperatures $C_Q(t)$ exhibits a two-step time-dependent decay similar to the self intermediate scattering function, and that the corresponding correlation time τ_Q displays a dynamic crossover from non-Arrhenius behavior for $T > T_W$ to Arrhenius behavior for $T < T_W$, where T_W denotes the Widom temperature where the correlation length has a maximum as T is decreased along a constant-pressure path. They defined a tetrahedral entropy S_Q associated with the local tetrahedral order of water molecules and find that it produces a major contribution to the specific heat maximum at the Widom line (Fig. 4), and showed that τ_Q can be extracted from S_Q using an analog of the Adam–Gibbs relation.

In his previous work, Kumar et al. [37–39] found similar results for a cell model of water, where the local tetrahedral order is defined by the states of discrete orientational bonding variables. They calculated, for both scenarios, the relaxation time τ of $S_i \equiv \sum_j \sigma_{ij}/4$, which quantifies the degree of total bond ordering for site i , where each molecule i has four bond indices $\sigma_{ij} \in [1, \dots, q=6]$, corresponding to the four n.n. cells j , each occupied by a water molecule, giving rise to $q^4 = 6^4 = 1296$ different molecular orientations. They associated the tetrahedral ordered configuration to the case when the four bond indices are in the same state. They identified τ as the time for the spin

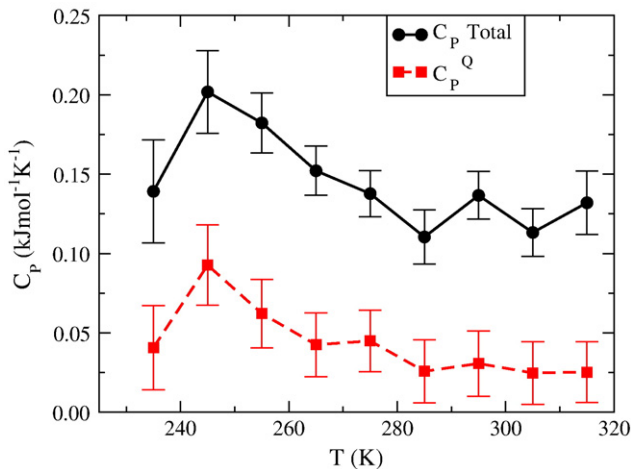


Fig. 4. Constant pressure specific heat C_p and specific heat associated with tetrahedral entropy C_p^Q of water at atmospheric pressure for TIP5P model of water.

autocorrelation function $C_{\sigma\sigma}(t) \equiv \langle S_i(t)S_i(0) \rangle / \langle S_i^2(0) \rangle$ to decay to the value $1/e$. They found that τ shows a crossover (Fig. 5a) from non-Arrhenius behavior for $T > T_W$ to an apparent Arrhenius behavior for $T < T_W$, where T_W is approximated with the temperature $T(C_p^{\text{max}})$ of the maximum of the isobaric specific heat C_p .

To prove that the dynamics is regulated by the structural changes, Kumar et al. proposed that E_1 , the lowest free energy excitation relevant at $T_W(P)$, is associated to the local rearrangement of a bond to assume a more tetrahedral (ordered) configuration. If the proposal is correct, then E_1 should correspond to the T -dependent activation energy $E_A = k_B T \log(\tau/\tau_0)$, where τ_0 is the unknown relaxation time for $T \rightarrow \infty$ and depends only on P . The results of their calculation is shown in Fig. 5b as lines, compared to the simulation results of Fig. 5a (symbols), with $\log \tau_0$ increasing with P as would be expected on the basis of a hard-sphere approximation, valid for $T \rightarrow \infty$. Hence, the calculations show that the mechanism to relax from a less structured state (low tetrahedral order) to a more structured state (higher tetrahedral order) corresponds to the breaking of a bond and the simultaneous molecular reorientation for the formation of a new bond.

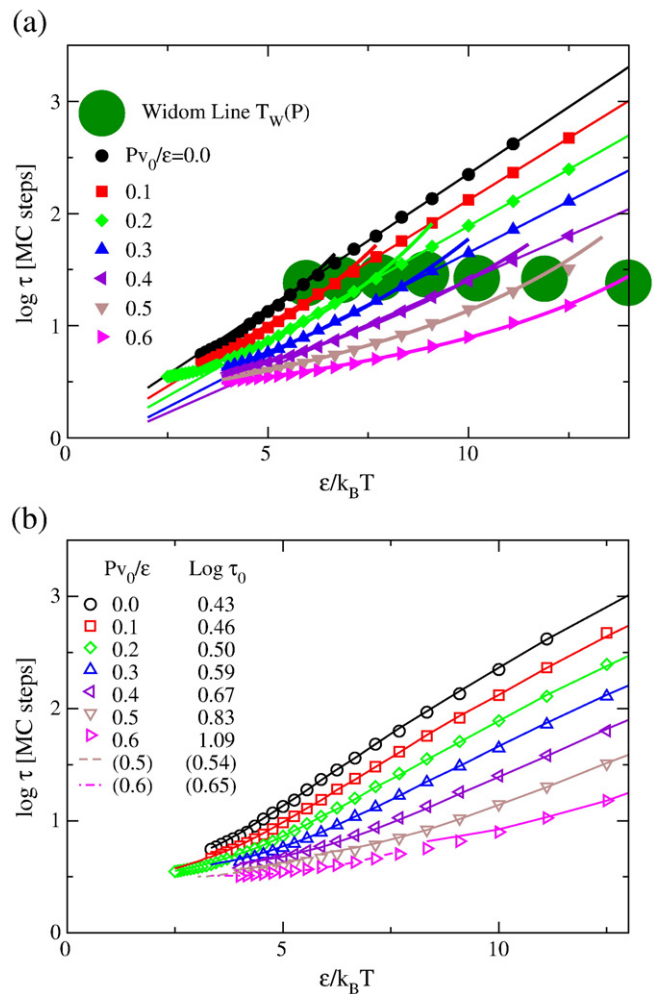


Fig. 5. (a) Dynamic crossover (large \oplus) in the tetrahedral order relaxation time τ for a range of different pressures, approaching the LLC critical P from below, with crossover temperature at $T_W(P) \approx T(C_p^{\text{max}})$. The error on $T_W(P)$ is approximately equal to symbol size; thick and thin lines represent VFT and Arrhenius fits. Notice that the dynamic crossover occurs at approximately the same value of τ for all seven values of pressure studied. P is expressed in internal units of the model. Lower panel: nd thin lines represent VFT and Arrhenius fits. (b) The theoretical prediction $E_1/k_B T + \log \tau_0$ (lines) describes well the $\log \tau$ from simulations (symbols) for $Pv_0/\epsilon = 0, 0.1, 0.2, 0.3, 0.4, 0.5, 0.6$. Only for the two largest values of P a deviation is observed at high T (dash and dot-dash lines) and $\log \tau = E_2/(k_B T) + \log \tau_0$ with $E_2 = -3E_{\text{IM}P_{\text{IM}}} - E_{\text{B}P_{\text{B}}}$ and $\log \tau_0$ given in the legend.

More recently, Mazza et al. [99,100] reached even more insight into this subject, by showing that the C_p^{\max} is determined by the maximum variation of the enthalpy associated to the formation of hydrogen bonds and that another crossover in the time-correlation function and another maximum of C_p occur at lower T . This lower- T maximum of C_p is due to the maximum variation of the enthalpy associated to the local tetrahedral order of water molecules and merges with the higher- T maximum of C_p when the pressure increases. These findings compare well with the dielectric spectroscopy experimental results of water molecules adsorbed onto lysozyme powder at low hydration level [100].

9. Selected results for bulk water

Using molecular dynamics (MD) simulations [101], Xu et al. [11] studied three models, each of which appears to have a liquid-liquid critical point. Two of the models (the TIP5P [102] and the ST2 [103]) treat water as a multiple site rigid body, interacting via electrostatic site-site interactions complemented by a Lennard-Jones potential. The third model is the spherical “two-scale” Jagla potential with attractive and repulsive ramps which has been studied in the context of liquid-liquid phase transitions and liquid anomalies [45,53,104,105]. For all three models, Xu et al. evaluated the loci of maxima of the relevant response functions, compressibility and specific heat, which coincide close to the critical point and give rise to the Widom line. They found evidence that, for all three potentials, the dynamic crossover occurs just when the Widom line is crossed.

Still another model has been studied, SPC/E, but the temperature shift is about 40 K since SPC/E is under-structured compared to real water as it collapses the two negatively charged lone pairs into a single negative point charge. Hence at such low temperatures the statistics are not very good for recognizing the critical point [106,107].

Other models, which are particularly tractable, include a family of spherically-symmetric potentials pioneered by Stell and Hemmer which are characterized by two length scales and hence reflect many of the properties of real water: see, e.g., [108–113].

These findings are consistent with the possibility that the observed dynamic crossover along path α of Fig. 2a is related to the behavior of C_p , suggesting that enthalpy or entropy fluctuations may have a strong influence on the dynamic properties [45,49,59]. Indeed, as the thermodynamic properties change from the high-temperature side of the Widom line to the low-temperature side, $(\partial S/\partial T)_p = C_p/T > 0$ implies that the entropy must decrease. The entropy decrease is most pronounced at the Widom line when $C_p = C_p^{\max}$. Since the configurational part of the entropy, S_{conf} , makes the major contribution to S , we expect that S_{conf} also decreases sharply on crossing the Widom line.

According to Adam-Gibbs theory [54], $D \sim \exp(-A/TS_{\text{conf}})$. Hence, we expect that D sharply decreases upon cooling at the Widom line. If S_{conf} does not change appreciably with T , then the Adam-Gibbs equation predicts an Arrhenius behavior of D . For both water and the Jagla model, crossing the Widom line is associated with the change in the behavior of the diffusivity. (i) In the case of water, D changes from non-Arrhenius to Arrhenius behavior, while the structural and thermodynamic properties change from those resembling HDL to those resembling LDL, due to the *negative* slope of the Widom line. (ii) For the Jagla potential, D changes from Arrhenius to non-Arrhenius while the structural and thermodynamic properties change from those resembling LDL to those resembling HDL, due to the *positive* slope of the Widom line.

Thus these results for bulk water are consistent with the experimental observation in confined water of (i) a fragility transition for $P < P_c$ [60,61], and (ii) a peak in C_p upon cooling water at atmospheric pressure [114], so this work offers a plausible interpretation of the results of Ref. [61] as supporting the existence of a hypothesized liquid-liquid critical point.

10. Glass transition in biomolecules

Next we explore, using MD simulations, the rather novel hypothesis [115] that the observed glass transition in biomolecules [116] is related to the liquid-liquid phase transition. Specifically, Kumar et al. [115] studied the dynamic and thermodynamic behavior of lysozyme and DNA in hydration TIP5P water, by means of the software package GROMACS for (i) an orthorhombic form of hen egg-white lysozyme and (ii) a Dickerson dodecamer DNA at constant pressure $P = 1$ atm, several constant temperatures T , and constant number of water molecules N (NPT ensemble).

Kumar et al. calculated the mean square fluctuations $\langle x^2 \rangle$ of the biomolecules from the equilibrated configurations, first for each atom over 1 ns, and then averaged over the total number of atoms in the biomolecule. They find that $\langle x^2 \rangle$ changes its functional form below $T_p \approx 245$ K, for *both* lysozyme and DNA.

Kumar et al. also calculated C_p by numerical differentiation of the total enthalpy of the system (protein and water) by fitting the simulation data for enthalpy with a fifth order polynomial, and then taking the derivative with respect to T . Fig. 6(a) and (b) display maxima of $C_p(T)$ at $T_w \approx 250 \pm 10$ K for both biomolecules.

Further, to describe the quantitative changes in structure of hydration water, Kumar et al. calculated the local tetrahedral order parameter Q [98,117–119] for hydration water surrounding lysozyme and DNA. Fig. 6(c) and (d) show that the rate of increase of Q has a maximum at 245 ± 10 K for lysozyme and DNA hydration water respectively; the same temperatures of the crossover in the behavior of mean square fluctuations.

Upon cooling, the diffusivity of hydration water exhibits a dynamic crossover from non-Arrhenius to Arrhenius behavior at the crossover temperature $T_x \approx 245 \pm 10$ K [Fig. 6(e)]. The coincidence of T_x with T_p within the error bars indicates that the behavior of the protein is strongly coupled with the behavior of the surrounding solvent, in agreement with recent experiments [116]. Note that T_x is much higher than the glass transition temperature, estimated for TIP5P as $T_g = 215$ K [120]. Thus this crossover is not likely to be related to the glass transition in water.

The fact that $T_p \approx T_x \approx T_w$ is evidence of the correlation between the changes in protein fluctuations and the hydration water thermodynamics [Fig. 6(a)]. Thus these results are consistent with the possibility that the protein glass transition is related to the Widom line (and hence to the hypothesized liquid-liquid critical point). Crossing the Widom line corresponds to a continuous but rapid transition of the properties of water from those resembling the properties of a local HDL structure for $T > T_w(P)$ to those resembling the properties of a local LDL structure for $T < T_w(P)$ [11,37–39,61]. A consequence is the expectation that the fluctuations of the protein residues in predominantly LDL-like water (more ordered and more rigid) just below the Widom line should be smaller than the fluctuations in predominantly HDL-like water (less ordered and less rigid) just above the Widom line.

The quantitative agreement of the results for both DNA and lysozyme is consistent with the interesting possibility that it is indeed the changes in the properties of hydration water that are responsible for the changes in dynamics of the protein and DNA biomolecules. Our results are in qualitative agreement with recent experiments on hydrated protein and DNA which found the crossover in side-chain fluctuations at $T_p \approx 225$ K.

11. Recent experiments using complementary experimental approaches

Complementary experimental approaches have been carried out by the Messina group of F. Mallamace and the MIT group of S.-H. Chen. The Chen et al. work using neutrons is discussed above. In this section

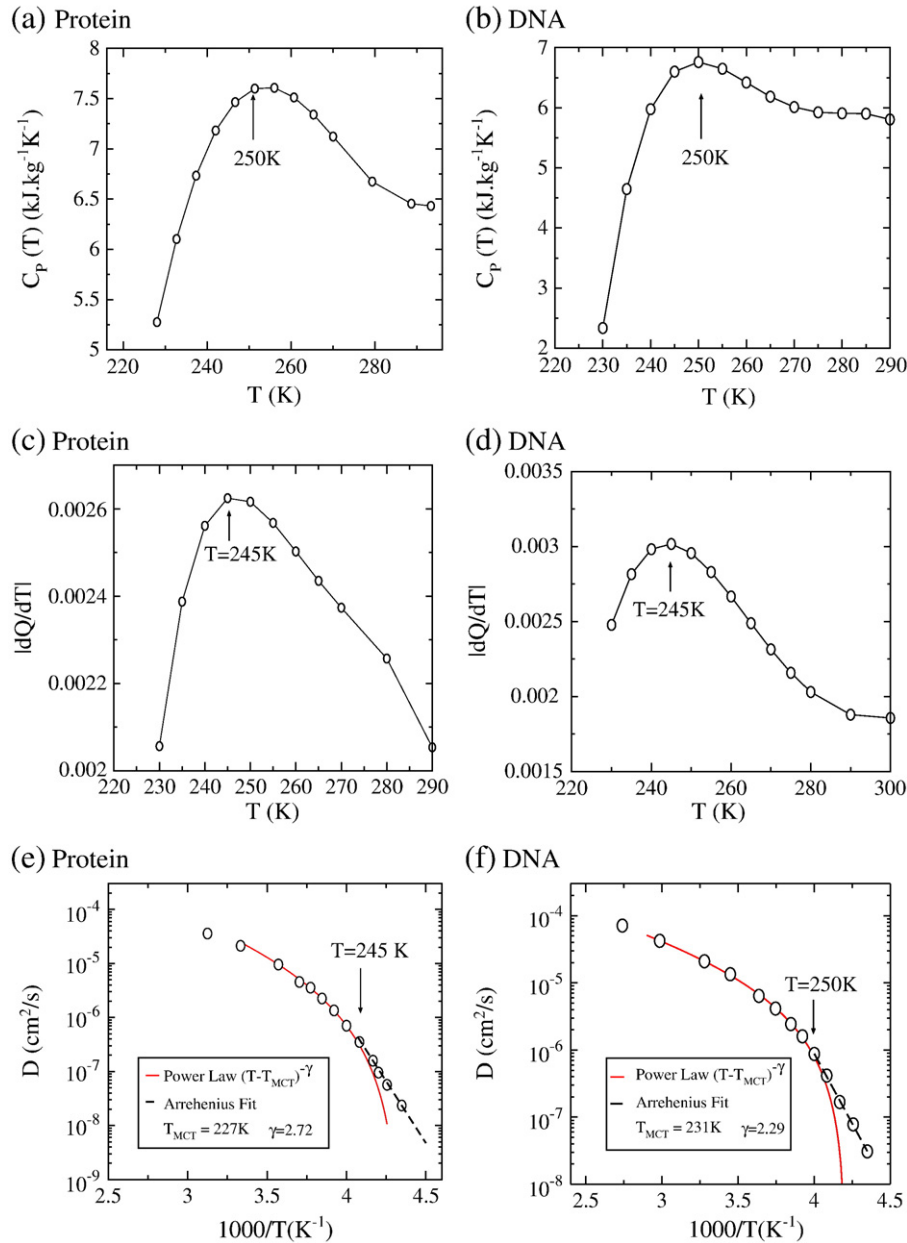


Fig. 6. The specific heat of the combined system (a) lysozyme and water, and (b) DNA and water, display maxima at 250 ± 10 K and 250 ± 12 K respectively, which are coincident within the error bars with the temperature T_p where the crossover in the behavior of $\langle x^2 \rangle$ is observed in the previous Figure. Derivative with respect to temperature of the local tetrahedral order parameter Q for (c) lysozyme and (d) DNA hydration water. A maximum in $|dQ/dT|$ at Widom line temperature suggests that the rate of change of local tetrahedrality of hydration water has a maximum at the Widom line. Diffusion constant of hydration water surrounding (e) lysozyme, and (f) DNA shows a dynamic transition from a power law behavior to an Arrhenius behavior at $T_{\times} \approx 245 \pm 10$ K for lysozyme and $T_{\times} \approx 250 \pm 10$ K for DNA, around the same temperatures where the behavior of $\langle x^2 \rangle$ has a crossover, and C_p and $|dQ/dT|$ have maxima.

we briefly mention some of the work of the Mallamace group, especially using NMR.

Figs. 7 and 8 deal with the equilibrium magnetization, $M_0(T)$ measured in water confined in MCM 41 micropores and the hydration water of the protein lysozyme. $M_0(T)$ is a quantity directly proportional to the magnetic susceptibility χ of a material under a static magnetic field H ($\chi = M_0/H$) that, in thermal equilibrium, is sensitive to the average angle between the direction of the atomic magnetic moment m and the applied field H . According to the Curie law, χ is related to the mean square value, per unit volume, of the nuclear magnetic moment and hence is sensitive to the local structural properties of the system. Details about the temperature behavior of $M_0(T)$ in confined supercooled water are reported in the reference [62]. In particular, the observed inflection point has been

attributed to the fragile-strong dynamical crossover observed in the T behavior of the self diffusion coefficient D_s and in the average translational relaxation time τ measured respectively by means of nuclear magnetic resonance and neutron scattering techniques. The inflection point temperature ($T_{\times} \approx 225$ K) is the same temperature below which water dynamics violates the Stokes–Einstein law.

Fig. 7 reports $M_0(T)$ for MCM samples of different nanotube sizes i.e.: 2.4, 1.8 and 1.4 nm measured in the cooling (C) and heating (H) experiments. Fig. 8 reports $M_0(T)$ measured in the lysozyme hydration water at the different protein concentrations: $h = 0.3; 0.37$ and 0.48 . One sees that the observed crossover temperature of protein hydration water is approximately the same of nanotube confined water.

Also reported in this issue is a demonstration that the fragile-strong crossover (observed with the same experimental approach)

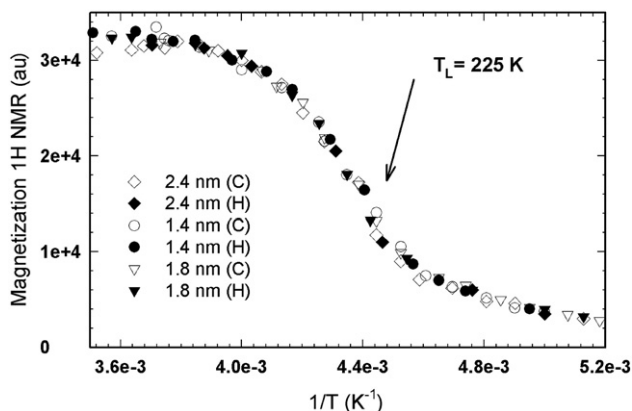


Fig. 7. NMR measurements of magnetization M_0 versus inverse T of hydrated lysozyme in MCM nanopores of three different diameters (1.4 nm, 1.8 nm, and 2.4 nm) measured upon cooling (C) or heating (H).

characterizes the supercooled state of many different glasses forming materials such as glycerol, salol and O-Terphenyl [121].

12. Outlook

It is possible that other phenomena that appear to occur on crossing the Widom line are in fact not coincidences, but are related to the changes in local structure that occur when the system changes from the “HDL-like” side to the “LDL-like” side of the Widom line. In this work we concentrated on reviewing the evidence (see, e.g., [122]) for changes in dynamic transport properties in both confined and bulk water—recognizing that the two systems are not identical, for indeed there is a rich literature concerning altogether new phenomena occurring in confined systems, as discussed in recent work of Han and collaborators [123–126] and references cited therein. Additional examples not discussed include: (1) a breakdown of the Stokes–Einstein relation for $T < T_W(P)$ [63,65,67,127–129], and possible relationships between these phenomena and properties of the hydrogen bond network [24] (2) systematic changes in the static structure factor $S(q)$ and the corresponding pair correlation function $g(r)$ revealing that for $T < T_W(P)$ the system more resembles the structure of LDL than HDL, (3) appearance for $T < T_W(P)$ of a shoulder in the dynamic structure factor $S(q, \omega)$ at a frequency $\omega \approx 60 \text{ cm}^{-1} \approx 2 \text{ THz}$ [116], a feature that we are currently

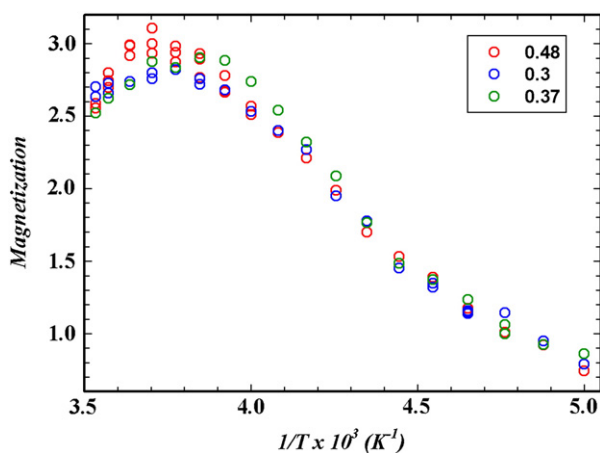


Fig. 8. The zero-field equilibrium magnetization, $M_0(T)$ measured in the lysozyme hydration water at two different concentrations (weight): $h = 0.3, 0.37$, and 0.48 . Data are corrected according to the Curie law. The behavior is analogous of water confined MCM nanotubes, i.e., in both the cases there is clear evidence that there is a steep decrease of $M_0(T)$ on decreasing T , at around $T_c = 225 \text{ K}$. This behavior represents another indication that $T = 225 \text{ K}$ is a crossover temperature for the dynamical behavior of water.

studying to test if it may be related to the appearance below the Widom line of a novel vibrational mode (a “Boson peak”), (4) rapid increase in hydrogen bonding degree for $T < T_W(P)$ [37], (5) a *minimum* in the density at low temperature [75,130], and (6) a scaled equation of state near the critical point [131]. It is important to know how general a given phenomenon is, such as crossing the Widom line which by definition is present whenever there is a critical point. Data on other liquids which have local tetrahedral symmetry, such as silicon and silica, appear to also display a liquid–liquid critical point and hence must possess a Widom line emanating from this point into the one-phase region. For example, Morishita interprets structural changes in silicon as arising from crossing the Widom line [132]. Underway are tests of the effect of the Widom line on simple model systems that display a liquid–liquid critical point, such as two-scale symmetric potentials of the sort recently studied by Xu et al. [45,133]. It is becoming clear that a local tetrahedral symmetry matters because it is associated with two characteristic length scales in the interaction potential. Other systems, such as metallic glasses, also appear to have two scale and there is evidence of polymorphism [134]. Finally, we mention the fact that there are many unsolved problems associated with what occurs when water dissolves a solute, and some of the approaches developed to understand the hypothesized liquid–liquid phase transition may be useful in addressing these problems [135–138].

Acknowledgments

This work has been carried out with many collaborators, of whom only a small number have joined this paper as co-authors. The work has been heavily influenced by a number of excellent experimentalists, including C. A. Angell [14], M. C. Bellissent-Funel [9], R. J. Birgeneau [139], L. Bosio [140], F. Bruni [100], S.-H. Chen [11,115,141], D. Leporini [142], L. Liu [61], F. Mallamace [143–147], O. Mishima [29,148,149], A. Nilsson [150,151], J. Teixeira [18,19] and by the very experienced computational chemist, A. Geiger [152,153]. The work at Boston University was supported by the Chemistry Division of the NSF. SVB thanks the Office of the Academic Affairs of Yeshiva University for funding the Yeshiva University high-performance computer cluster and acknowledges the partial support of this research through the Dr. Bernard W. Gamson Computational Science Center at Yeshiva College. GF thanks the Spanish Ministerio de Ciencia e Innovación grant FIS2009–10210 (co-financed FEDER). XLM acknowledges the support by the World Premier International Research Center Initiative (WPI Initiative), MEXT, Japan.

References

- [1] G. Franzese, H.E. Stanley, Understanding the properties of water, in: R.M. Lynden-Bell, S. Conway Morris, J.D. Barrow, J.L. Finney, C. Harper (Eds.), *Water and Life: The Unique Properties of H₂O*, Taylor and Francis, Boca Raton, 2010, pp. 99–114, Chapter 8.
- [2] E.A. Zheligovskaya, G.G. Malenkov, *Crystalline water ices*, *Russ. Chem. Rev.* 75 (2006) 57–76.
- [3] P.G. Debenedetti, Supercooled and glassy water, *J. Phys.: Condens. Matter* 15 (2003) R1669–R1726.
- [4] T. Loerting, N. Giovambattista, Amorphous ices: experiments and numerical simulations, *J. Phys.: Condens. Matter* 18 (2006) R919–R977.
- [5] C.U. Kim, B. Barstow, M.W. Tate, S.M. Gruner, Evidence for liquid water during the high-density to low-density amorphous ice transition, *Proc. Natl. Acad. Sci. USA* 106 (2009) 4596–4600.
- [6] C.A. Angell, in: F. Franks (Ed.), *Water: A Comprehensive Treatise*, Vol. 7, Plenum, New York, 1982, pp. 1–81, [29].
- [7] R.J. Speedy, Limiting forms of the thermodynamic divergences at the conjectured stability limits in superheated and supercooled water, *J. Phys. Chem.* 86 (1982) 3002–3005.
- [8] P.H. Poole, F. Sciortino, U. Essmann, H.E. Stanley, Phase behavior of metastable water, *Nature* 360 (1992) 324–328.
- [9] F.W. Starr, M.-C. Bellissent-Funel, H.E. Stanley, Continuity of liquid and glassy water, *Phys. Rev. E* 60 (1999) 1084–1087.
- [10] M.C. Bellissent-Funel, L. Bosio, A neutron scattering study of liquid D₂O, *J. Chem. Phys.* 102 (1995) 3727–3735.
- [11] L. Xu, P. Kumar, S.V. Buldyrev, S.-H. Chen, P.H. Poole, F. Sciortino, H.E. Stanley, Relation between the Widom line and the dynamic crossover in systems with a liquid–liquid critical point, *Proc. Natl. Acad. Sci.* 102 (2005) 16558–16562.

- [12] G. Franzese, H.E. Stanley, The Widom line of supercooled water, *J. Phys.: Condens. Matter* 19 (2007) 205126.
- [13] F. Sciortino, P.H. Poole, U. Essmann, H.E. Stanley, Line of compressibility maxima in the phase diagram of supercooled water, *Phys. Rev. E* 55 (1997) 727–737.
- [14] P.H. Poole, F. Sciortino, T. Grande, H.E. Stanley, C.A. Angell, Effect of hydrogen bonds on the thermodynamic behavior of liquid water, *Phys. Rev. Lett.* 73 (1994) 1632–1635.
- [15] H. Tanaka, A self-consistent phase diagram for supercooled water, *Nature* 380 (1996) 328–330.
- [16] H. Tanaka, Phase behaviors of supercooled water: reconciling a critical point of amorphous ices with spinodal instability, *J. Chem. Phys.* 105 (1996) 5099–5111.
- [17] S. Sastry, P. Debenedetti, F. Sciortino, H.E. Stanley, Singularity-free interpretation of the thermodynamics of supercooled water, *Phys. Rev. E* 53 (1996) 6144–6154.
- [18] H.E. Stanley, A polychromatic correlated-site percolation problem with possible relevance to the unusual behavior of supercooled H₂O and D₂O, *J. Phys. A* 12 (1979) L329–L337.
- [19] H.E. Stanley, J. Teixeira, Interpretation of the unusual behavior of H₂O and D₂O at low temperatures: tests of a percolation model, *J. Chem. Phys.* 73 (1980) 3404–3422.
- [20] C.A. Angell, Insights into phases of liquid water from study of its unusual glass-forming properties, *Science* 319 (2008) 582–587.
- [21] P.A. Netz, F.W. Starr, H.E. Stanley, M.C. Barbosa, Static and dynamic properties of stretched water, *J. Chem. Phys.* 115 (2001) 344–348.
- [22] F.W. Starr, J.K. Nielsen, H.E. Stanley, Fast and slow dynamics of hydrogen bonds in liquid water, *Phys. Rev. Lett.* 82 (1999) 2294–2297.
- [23] F.W. Starr, J.K. Nielsen, H.E. Stanley, Hydrogen bond dynamics for the extended simple point charge model of water, *Phys. Rev. E* 62 (2000) 579–587.
- [24] F. Sciortino, P. Poole, H.E. Stanley, S. Havlin, Lifetime of the hydrogen bond network and gel-like anomalies in supercooled water, *Phys. Rev. Lett.* 64 (1990) 1686–1689.
- [25] S.S. Borick, P.G. Debenedetti, S. Sastry, A lattice model of network-forming fluids with orientation-dependent bonding: equilibrium, stability, and implications from the phase behavior of supercooled water, *J. Phys. Chem.* 99 (1995) 3781–3793.
- [26] T.M. Truskett, P.G. Debenedetti, S. Sastry, S. Torquato, A single-bond approach to orientation-dependent interactions and its implications for liquid water, *J. Chem. Phys.* 111 (1999) 2647–2656.
- [27] H. Tanaka, Thermodynamic anomaly and polymorphism of water, *Europhys. Lett.* 50 (2000) 340–346.
- [28] K. Stokely, M.G. Mazza, H.E. Stanley, G. Franzese, Effect of hydrogen bond cooperativity on the behavior of water, *Proc. Natl. Acad. Sci. USA* 107 (2010) 1301–1306.
- [29] O. Mishima, H.E. Stanley, Decompression-induced melting of ice iv and the liquid–liquid transition in water, *Nature* 392 (1998) 164–168.
- [30] O. Mishima, Liquid–liquid critical point in heavy water, *Phys. Rev. Lett.* 85 (2000) 334–336.
- [31] F. Mallamace, M. Broccio, C. Corsaro, A. Faraone, D. Majolino, V. Venuti, L. Liu, C.Y. Mou, S.-H. Chen, Evidence of the existence of the low-density liquid phase in supercooled, confined water, *Proc. Natl. Acad. Sci. USA* 104 (2007) 424–428.
- [32] M.A. Anisimov, J.V. Sengers, J.M.H. Levelt Sengers, Near-critical behavior of aqueous systems, in: D.A. Palmer, R. Fernandez-Prini, A.H. Harvey (Eds.), *Aqueous System at Elevated Temperatures and Pressures: Physical Chemistry in Water, Steam and Hydrothermal Solutions*, Elsevier, Amsterdam, 2004.
- [33] U. Raviv, P. Laurat, J. Klein, Fluidity of water confined to subnanometre films, *Nature* 413 (2001) 51–54.
- [34] G. Franzese, H.E. Stanley, Liquid–liquid critical point in a Hamiltonian model for water: analytic solution, *J. Phys.: Condens. Matter* 14 (2002) 2201–2209.
- [35] G. Franzese, H.E. Stanley, A theory for discriminating the mechanism responsible for the water density anomaly, *Physica A* 314 (2002) 508.
- [36] G. Franzese, M.I. Marqués, H.E. Stanley, Intramolecular coupling as a mechanism for a liquid–liquid phase transition, *Phys. Rev. E* 67 (2003) 011103.
- [37] P. Kumar, G. Franzese, H.E. Stanley, Predictions of dynamic behavior under pressure for two scenarios to explain water anomalies, *Phys. Rev. Lett.* 100 (2008) 105701.
- [38] P. Kumar, G. Franzese, H.E. Stanley, Dynamics and thermodynamics of water, *J. Phys.: Condens. Matter* 20 (2008) 244114.
- [39] P. Kumar, G. Franzese, S.V. Buldyrev, H.E. Stanley, Dynamics of water at low temperatures and implications for biomolecules, in: G. Franzese, M. Rubi (Eds.), *Aspects of Physical Biology. Biological Water, Protein Solutions, Transport and Replication*, Lecture Notes in Physics, 752, Springer, Berlin, 2008.
- [40] F.-F. Li, Q.-L. Cui, Z. He, J. Zhang, Q. Zhou, G.-T. Zou, High pressure–temperature Brillouin study of liquid water: evidence of the structural transition from low-density water to high-density water, *J. Chem. Phys.* 123 (2005) 174511.
- [41] G. Franzese, K. Stokely, X.-Q. Chu, P. Kumar, M.G. Mazza, S.-H. Chen, H.E. Stanley, Pressure effects in supercooled water: comparison between a 2D model of water and experiments for surface water on a protein, *J. Phys.: Condens. Matter* 20 (2008) 494210.
- [42] X.-Q. Chu, A. Faraone, C. Kim, E. Fratini, P. Baglioni, J.B. Leao, S.-H. Chen, Proteins remain soft at lower temperatures under pressure, *J. Phys. Chem. B* 113 (2009) 5001–5006.
- [43] P.G. Debenedetti, H.E. Stanley, The physics of supercooled and glassy water, *Phys. Today* 56 (issue 6) (2003) 40–46.
- [44] J.M.H. Levelt, Measurements of the Compressibility of Argon in the Gaseous and Liquid Phase, Ph.D. Thesis (University of Amsterdam, Van Gorkum and Co., 1958).
- [45] L. Xu, S.V. Buldyrev, C.A. Angell, H.E. Stanley, Thermodynamics and dynamics of the two-scale spherically symmetric Jagla ramp model of anomalous liquids, *Phys. Rev. E* 74 (2006) 031108.
- [46] F. Mallamace, The liquid water polymorphism, *Proc. Natl. Acad. Sci. USA* 106 (2009) 15097–15098.
- [47] G.G. Simeoni, T. Bryk, F.A. Gorelli, M. Krisch, G. Ruocco, M. Santoro, T. Scopigno, The Widom line as the crossover between liquid-like and gas-like behaviour in supercritical fluids, *Nat. Phys.* 6 (2010) 503–507.
- [48] P.F. McMillan, H.E. Stanley, Going supercritical, *Nat. Phys.* 6 (2010) 479–480.
- [49] F.W. Starr, C.A. Angell, H.E. Stanley, Prediction of entropy and dynamic properties of water below the homogeneous nucleation temperature, *Physica A* 323 (2003) 51–66.
- [50] P. Kumar, S.V. Buldyrev, F. Starr, N. Giovambattista, H.E. Stanley, Thermodynamics, structure, and dynamics of water confined between hydrophobic plates, *Phys. Rev. E* 72 (2005) 051503.
- [51] G. Franzese, F. de los Santos, Dynamically slow processes in supercooled water confined between hydrophobic plates, *J. Phys.: Condens. Matter* 21 (2009) 504107.
- [52] G. Franzese, A. Hernando-Martínez, P. Kumar, M.G. Mazza, K. Stokely, E.G. Strelakova, F. Santos, H.E. Stanley, Phase transitions and dynamics in bulk and interfacial water [Proc. Lausanne CECAM Conference], *J. Phys. Condensed Matter* 22 (2010) 284103.
- [53] E.A. Jagla, Core-softened potentials and the anomalous properties of water, *J. Chem. Phys.* 111 (1999) 8980–8986.
- [54] G. Adam, J.H. Gibbs, On the temperature dependence of cooperative relaxation properties in glass-forming liquids, *J. Chem. Phys.* 43 (1965) 139–146.
- [55] P.H. Poole, I. Saika-Voivod, F. Sciortino, Density minimum and liquid–liquid phase transition, *J. Phys.: Condens. Matter* 17 (2005) L431–L437.
- [56] S. Sastry, C.A. Angell, Liquid–liquid phase transition in supercooled silicon, *Nat. Mater.* 2 (2003) 739–743.
- [57] P. Ganesh, M. Widom, Liquid–liquid transition in supercooled silicon determined by first-principles simulation, *Phys. Rev. Lett.* 102 (2009) 075701.
- [58] M. Beye, F. Sorgenfrei, W.F. Schlotter, W. Wurth, A. Frisch, The liquid–liquid phase transition in silicon revealed by snapshots of valence electrons, *Proc. Natl. Acad. Sci.* 107 (2010) 16772–26776.
- [59] I. Saika-Voivod, P.H. Poole, F. Sciortino, Fragile-to-strong transition and polymorphism in the energy landscape of liquid silica, *Nature* 412 (2001) 514–517.
- [60] A. Faraone, L. Liu, C.-Y. Mou, C.-W. Yen, S.-H. Chen, Fragile-to-strong liquid transition in deeply supercooled confined water, *J. Chem. Phys.* 121 (2004) 10843–10846.
- [61] L. Liu, S.-H. Chen, A. Faraone, C.-W. Yen, C.Y. Mou, Pressure dependence of fragile-to-strong transition and a possible second critical point in supercooled confined water, *Phys. Rev. Lett.* 95 (2005) 117802.
- [62] F. Mallamace, M. Broccio, C. Corsaro, A. Faraone, U. Wanderlingh, L. Liu, C.Y. Mou, S.-H. Chen, The fragile-to-strong dynamic crossover transition in confined water: nuclear magnetic resonance results, *J. Chem. Phys.* 124 (2006) 161102.
- [63] L. Xu, F. Mallamace, Z. Yan, F.W. Starr, S.V. Buldyrev, H.E. Stanley, Appearance of a fractional Stokes–Einstein relation in water and a structural interpretation of its onset, *Nat. Phys.* 5 (2009) 565–569.
- [64] F. Mallamace, C. Branca, C. Corsaro, N. Leone, J. Spooren, S.-H. Chen, H.E. Stanley, Transport properties of glass-forming liquids suggest the dynamic crossover temperature is as important as the glass transition temperature, *Proc. Natl. Acad. Sci. USA* 107 (2010) 22457–22462.
- [65] S.-H. Chen, F. Mallamace, C.-Y. Mou, M. Broccio, C. Corsaro, A. Faraone, L. Liu, The violation of the Stokes–Einstein relation in supercooled water, *Proc. Natl. Acad. Sci. USA* 103 (2006) 12974–12978.
- [66] S.R. Becker, P.H. Poole, F.W. Starr, Fractional Stokes–Einstein and Debye–Stokes–Einstein relations in a network-forming liquid, *Phys. Rev. Lett.* 97 (2006) 055901.
- [67] M.G. Mazza, N. Giovambattista, H.E. Stanley, F.W. Starr, Breakdown of the Stokes–Einstein and Stokes–Einstein–Debye relations and dynamics heterogeneities in a molecular system, *Phys. Rev. E* 76 (2007) 031203.
- [68] F. Fernandez-Alonso, F.J. Bermejo, S.E. McLain, J.F.C. Turner, J.J. Molaison, K.W. Herwig, Observation of fractional Stokes–Einstein behavior in the simplest hydrogen-bonded liquid, *Phys. Rev. Lett.* 98 (2007) 077801.
- [69] J.F. Douglas, D. Leporini, Obstruction model of the fractional Stokes–Einstein relation in glass-forming liquids, *J. Non-Cryst. Sol.* 235 (1998) 137–141.
- [70] A.K. Soper, M.A. Ricci, Structures of high-density and low-density water, *Phys. Rev. Lett.* 84 (2000) 2881–2884.
- [71] J.M. Zanotti, M.C. Bellissent-Funel, S.-H. Chen, Experimental evidence of a liquid–liquid transition in interfacial water, *Europhys. Lett.* 71 (2005) 91–97.
- [72] G.E. Walrafen, M.S. Hokmabadi, W.H.A. Yang, Raman isosbestic points from liquid water, *J. Chem. Phys.* 85 (1986) 6964–6969.
- [73] M. Canpolat, F.W. Starr, M.R. Sadr-Lahijany, A. Scala, O. Mishima, S. Havlin, H.E. Stanley, Local structural heterogeneities in liquid water under pressure, *Chem. Phys. Lett.* 294 (1998) 9–12.
- [74] M.G. Mazza, K. Stokely, E.G. Strelakova, H.E. Stanley, G. Franzese, Cluster Monte Carlo and numerical mean field analysis for the water liquid–liquid phase transition, *Comp. Phys. Comm.* 180 (2009) 497–502.
- [75] R. Mancinelli, F. Bruni, M.A. Ricci, Controversial evidence on the point of minimum density in deeply supercooled confined water, *J. Phys. Chem. Lett.* 1 (2010) 1277–1282.
- [76] G.H. Findenegg, S. Jaehnert, D. Akcakayiran, A. Schreiber, Freezing and melting of water confined in silica nanopores, *ChemPhysChem* 9 (2008) 2651–2659.
- [77] N. Giovambattista, P.J. Rossky, P.G. Debenedetti, Effect of pressure on the phase behavior and structure of water confined between nanoscale hydrophobic and hydrophilic plates, *Phys. Rev. E* 73 (2006) 041604.

- [78] K. Morishige, K. Nobuoka, X-ray diffraction studies of freezing and melting of water confined in a mesoporous adsorbent (MCM-41), *J. Chem. Phys.* 107 (1997) 6965–6969.
- [79] A. Schreiber, A. Schreiber, I. Ketelsen, G.H. Findeneegg, Melting and freezing of water in ordered mesoporous silica materials, *Phys. Chem. Chem. Phys.* 3 (2001) 1185–1195.
- [80] P. Gallo, M. Rovere, S.-H. Chen, Dynamic crossover in supercooled confined water: understanding bulk properties through confinement, *J. Phys. Chem. Lett.* 1 (2010) 729–733.
- [81] P. Gallo, A. Attili, M. Rovere, Mode-coupling behavior of a Lennard–Jones binary mixture upon increasing confinement, *Phys. Rev. E* 80 (2009) 061502.
- [82] V. De Grandis, P. Gallo, M. Rovere, The phase diagram of confined fluids [European/Japanese Molecular Liquids Groups Interdisciplinary Conference, Sept. 04–08, 2005 Prague], *J. Mol. Liq.* 134 (2007) 90–93.
- [83] V. De Grandis, P. Gallo, M. Rovere, Liquid–liquid coexistence in the phase diagram of a fluid confined in fractal porous materials, *Europhys. Lett.* 75 (2006) 901–907.
- [84] A. Attili, P. Gallo, M. Rovere, Mode coupling behavior of a Lennard–Jones binary mixture: a comparison between bulk and confined phases, *J. Chem. Phys.* 123 (2005) 174510.
- [85] P. Gallo, A. Attili, M. Rovere, Slow dynamics of a confined supercooled binary mixture in comparison with the bulk phase [9th International Workshop on Disordered Systems, Mar. 10–13, 2003 Molveno Andalo, Italy], *Philos. Mag.* 84 (2004) 1397–1404.
- [86] P. Gallo, R. Pellarin, M. Rovere, Slow dynamics of a confined supercooled binary mixture: II. Q space analysis, *Phys. Rev. E* 68 (2003) 061209.
- [87] P. Gallo, M. Rovere, Anomalous dynamics of confined water at low hydration, *J. Phys.-Cond. Mat.* 15 (2003) 7625–7633.
- [88] A. Attili, P. Gallo, M. Rovere, Inherent structures and Kauzmann temperature of confined liquids, *Phys. Rev. E* 71 (2005) 031204.
- [89] P. Gallo, M. Rovere, Double dynamical regime of confined water, *J. Phys.-Cond. Mat.* 15 (2003) 1521–1529.
- [90] M. Rovere, P. Gallo, Effects of confinement on static and dynamical properties of water, *Eur. Phys. J. E* 12 (2003) 77–81.
- [91] M. Yamada, S. Mossa, H.E. Stanley, F. Sciortino, Interplay between time-temperature-transformation and the liquid–liquid phase transition in water, *Phys. Rev. Lett.* 88 (2002) 195701.
- [92] M.G. Mazza, N. Giovambattista, F.W. Starr, H.E. Stanley, Relation between rotational and translational dynamic heterogeneities in water, *Phys. Rev. Lett.* 96 (2006) 057803.
- [93] P. Kumar, S.V. Buldyrev, H.E. Stanley, A tetrahedral entropy for water, *Proc. Natl. Acad. Sci. USA* 106 (2009) 22130–22134.
- [94] F. Sciortino, A. Geiger, H.E. Stanley, Effect of defects on molecular mobility in liquid water, *Nature* 354 (1991) 218–221.
- [95] N. Giovambattista, F.W. Starr, S. Sciortino, S.V. Buldyrev, H.E. Stanley, Transitions between inherent structures in water, *Phys. Rev. E* 65 (2002) 041502.
- [96] V. Molinero, E.B. Moore, Water modeled as an intermediate element between carbon and silicon, *J. Phys. Chem. B* 113 (2009) 4008–4016.
- [97] E.B. Moore, V. Molinero, Growing correlation length in supercooled water, *J. Chem. Phys.* 130 (2009) 244505.
- [98] J.R. Errington, P.G. Debenedetti, Relationship between structural order and the anomalies of liquid water, *Nature* 409 (2001) 318–321.
- [99] M.G. Mazza, K. Stokely, H.E. Stanley, G. Franzese, “Anomalous specific heat of supercooled water,” arXiv:0807.4267 (2008).
- [100] M.G. Mazza, K. Stokely, S.E. Pagnotta, F. Bruni, H.E. Stanley, G. Franzese, “Two dynamic crossovers in protein hydration water and their thermodynamic interpretation,” arXiv:0907.1810v1 (2009).
- [101] D.C. Rapaport, *The Art of Molecular Dynamics Simulation*, Cambridge University Press, Cambridge, 1995.
- [102] M.W. Mahoney, W.L. Jorgensen, A five-site model for liquid water and the reproduction of the density anomaly by rigid, nonpolarizable potential functions, *J. Chem. Phys.* 112 (2000) 8910–8922.
- [103] F.H. Stillinger, A. Rahman, Molecular dynamics study of temperature effects on water structure and kinetics, *J. Chem. Phys.* 57 (1972) 1281–1292.
- [104] P. Kumar, S.V. Buldyrev, F. Sciortino, E. Zaccarelli, H.E. Stanley, Static and dynamic anomalies in a repulsive spherical ramp liquid: theory and simulation, *Phys. Rev. E* 72 (2005) 021501.
- [105] L. Xu, I. Ehrenberg, S.V. Buldyrev, H.E. Stanley, Relationship between the liquid–liquid phase transition and dynamic behavior in the Jagla model, *J. Phys.: Condens. Matter* 18 (2006) S2239–S2246.
- [106] S. Harrington, P.H. Poole, F. Sciortino, H.E. Stanley, Equation of state of supercooled SPC/E water, *J. Chem. Phys.* 107 (1997) 7443–7450.
- [107] P. Kumar, G. Franzese, S.V. Buldyrev, H.E. Stanley, Molecular dynamics study of orientational cooperativity in water, *Phys. Rev. E* 73 (2006) 041505.
- [108] M.R. Sadr-Lahijany, A. Scala, S.V. Buldyrev, H.E. Stanley, Liquid state anomalies for the Stell–Hemmer core-softened potential, *Phys. Rev. Lett.* 81 (1998) 4895–4898.
- [109] G. Franzese, G. Malescio, A. Skibinsky, S.V. Buldyrev, H.E. Stanley, Generic mechanism for generating a liquid–liquid phase transition, *Nature* 409 (2001) 692–695 cond-mat/0102029.
- [110] G. Franzese, Differences between discontinuous and continuous soft-core attractive potentials: the appearance of density anomaly, *J. Mol. Liq.* 136 (2007) 267.
- [111] A.B. de Oliveira, G. Franzese, P.A. Netz, M.C. Barbosa, Waterlike hierarchy of anomalies in a continuous spherical shouldered potential, *J. Chem. Phys.* 128 (2008) 064901.
- [112] P. Vilaseca, G. Franzese, Softness dependence of the Anomalies for the Continuous Shouldered Well potential, *J. Chem. Phys.* 133 (2010) 084507.
- [113] E. Lascaris, G. Malescio, S.V. Buldyrev, H.E. Stanley, Cluster formation, waterlike anomalies, and re-entrant melting for a family of bounded repulsive interaction potentials, *Phys. Rev. E* 81 (2010) 031201.
- [114] S. Maruyama, K. Wakabayashi, M. Oguni, Thermal properties of supercooled water confined within silica gel pores, *AIP Conf. Proc.* 708 (2004) 675–676.
- [115] P. Kumar, Z. Yan, L. Xu, M.G. Mazza, S.V. Buldyrev, S.-H. Chen, S. Sastry, H.E. Stanley, Glass transition in biomolecules and the liquid–liquid critical point of water, *Phys. Rev. Lett.* 97 (2006) 177802.
- [116] S.-H. Chen, L. Liu, E. Fratini, P. Baglioni, A. Faraone, E. Mamontov, The observation of fragile-to-strong dynamic crossover in protein hydration water, *Proc. Natl. Acad. Sci. USA* 103 (2006) 9012.
- [117] Z. Yan, S.V. Buldyrev, N. Giovambattista, H.E. Stanley, Structural order for one-scale and two-scale potentials, *Phys. Rev. Lett.* 95 (2005) 130604.
- [118] Z. Yan, S.V. Buldyrev, N. Giovambattista, P.G. Debenedetti, H.E. Stanley, Family of tunable spherically-symmetric potentials that span the range from hard spheres to water-like behavior, *Phys. Rev. E* 73 (2006) 051204.
- [119] Z. Yan, S.V. Buldyrev, P. Kumar, N. Giovambattista, P.G. Debenedetti, H.E. Stanley, Structure of the first- and second-neighbor shells of simulated water: quantitative relation to translational and orientational order, *Phys. Rev. E* 76 (2007) 051201.
- [120] I. Brovchenko, A. Geiger, A. Oleinikova, Liquid–liquid phase transitions in supercooled water studied by computer simulations of various water models, *J. Chem. Phys.* 123 (2005) 044515.
- [121] F. Mallamace, C. Branca, C. Corsaro, J. Spooren, S.-H. Chen, H.E. Stanley, Thermodynamical properties of glass forming systems: a nuclear magnetic resonance analysis, *Proc. 6th International Conference on Relaxation Phenomena in Complex systems (Rome)*, *J. Non-Cryst. Solids*, 357, 2011, pp. 286–292.
- [122] F. Mallamace, C. Branca, M. Broccio, C. Corsaro, N. Gonzalez-Segredo, H.E. Stanley, S.-H. Chen, Transport properties of supercooled confined water, *Proc. International Conf. on Transport, Localization, and Fluctuations in Complex Systems*, *European Physical Journal: Special Topics*, 161, 2008, pp. 19–33.
- [123] S. Han, M.Y. Choi, P. Kumar, H.E. Stanley, Phase transitions in confined water films, *Nat. Phys.* 6 (2010) 685–689.
- [124] S. Han, P. Kumar, H.E. Stanley, Absence of a diffusion anomaly of water in the direction perpendicular to hydrophobic nanoconfining walls, *Phys. Rev. E* 77 (3) (2008) 030201(R).
- [125] P. Kumar, S. Han, H.E. Stanley, Anomalies of water and hydrogen bond dynamics in hydrophobic nanoconfinement [Proc. Taormina Conference – Dedicated to Professor Francesco Mallamace, University of Messina, on the occasion of his 60th birthday], *J. Phys. Condens. Matter* 21 (2009) 504108.
- [126] S. Han, P. Kumar, H.E. Stanley, Hydrogen-bond dynamics of water in a quasi-two-dimensional hydrophobic nanopore slit, *Phys. Rev. E* 79 (2009) 041202.
- [127] P. Kumar, S.V. Buldyrev, S.L. Becker, P.H. Poole, F.W. Starr, H.E. Stanley, Relation between the Widom line and the Breakdown of the Stokes–Einstein relation in supercooled water, *Proc. Natl. Acad. Sci.* 104 (2007) 9575–9579.
- [128] P.A. Netz, F. Starr, M.C. Barbosa, H.E. Stanley, Translational and rotational diffusion in stretched water, *J. Molec. Liquids* 101 (2002) 159–168.
- [129] F. Mallamace, C. Branca, C. Corsaro, N. Leone, J. Spooren, H.E. Stanley, S.-H. Chen, Dynamical crossover and breakdown of the Stokes–Einstein relation in confined water and in methanol-diluted bulk water, *J. Phys. Chem. B* 114 (2010) 1870–1878.
- [130] D. Liu, Y. Zhang, C.-C. Chen, C.-Y. Mou, P.H. Poole, S.-H. Chen, Observation of the density minimum in deeply supercooled confined water, *Proc. Natl. Acad. Sci.* 104 (2007) 9570–9574.
- [131] D.A. Fuentevilla, M.A. Anisimov, Scaled equation of state for supercooled water near the liquid–liquid critical point, *Phys. Rev. Lett.* 97 (2006) 195702.
- [132] T. Morishita, How does tetrahedral structure grow in liquid silicon on supercooling? *Phys. Rev. Lett.* 97 (2006) 165502.
- [133] L. Xu, S.V. Buldyrev, N. Giovambattista, C.A. Angell, H.E. Stanley, A monatomic system with a liquid–liquid critical point and two distinct glassy states, *J. Chem. Phys.* 130 (2009) 054505.
- [134] H.W. Sheng, H.Z. Liu, Y.Q. Cheng, J. Wen, P.L. Lee, W.K. Luo, S.D. Shastri, E. Ma, Polyamorphism in a metallic glass, *Nat. Mater.* 6 (2007) 192–197.
- [135] S.V. Buldyrev, P. Kumar, P.G. Debenedetti, P. Rossky, H.E. Stanley, Water-like solvation thermodynamics in a spherically-symmetric solvent model with two characteristic lengths, *Proc. Natl. Acad. Sci.* 104 (2007) 20177–20182.
- [136] D. Corradini, S.V. Buldyrev, P. Gallo, H.E. Stanley, Effects of hydrophobic solutes on the liquid–liquid critical point, *Phys. Rev. E* 81 (2010) 061504.
- [137] S.V. Buldyrev, P. Kumar, S. Sastry, H.E. Stanley, S. Weiner, Hydrophobic collapse and cold denaturation in the Jagla model of water [Proc. Lausanne CECAM Conference], *J. Phys. Condens. Matter* 22 (2010) 284109.
- [138] M.I. Marqués, J.M. Borreguero, H.E. Stanley, N.V. Dokholyan, A possible mechanism for cold denaturation of proteins at high pressure, *Phys. Rev. Lett.* 91 (2003) 138103.
- [139] H.E. Stanley, R.J. Birgeneau, P.J. Reynolds, J.F. Nicoll, Thermally driven phase transitions near the percolation threshold in two dimensions, *J. Phys. C: Solid State Phys.* 9 (1976) L553–L560.
- [140] L. Bosio, J. Teixeira, H.E. Stanley, Enhanced density fluctuations in supercooled H₂O, D₂O, and ethanol–water solutions: evidence from small-angle X-ray scattering, *Phys. Rev. Lett.* 46 (1981) 597–600.
- [141] Y. Zhang, A. Faraone, W.A. Kamitakahara, K.-H. Liu, C.-Y. Mou, S.-H. Chen, Experimental Evidence of the Existence of a Liquid–Liquid Critical Point in Supercooled Confined Water, *Phys. Rev. Lett.* (in press).

- [142] D. Banerjee, S.N. Bhat, S.V. Bhat, D. Leporini, ESR evidence for two coexisting liquid phases in deeply supercooled bulk water, *Proc. Natl. Acad. Sci. USA* 106 (2009) 11448–11453.
- [143] F. Mallamace, M. Broccio, C. Corsaro, A. Faraone, D. Majolino, V. Venuti, L. Liu, C.-Y. Mou, S.H. Chen, Evidence of the existence of the low-density liquid phase in supercooled, confined water, *Proc. Natl. Acad. Sci.* 104 (2007) 424–428.
- [144] F. Mallamace, S.-H. Chen, M. Broccio, C. Corsaro, V. Crupi, D. Majolino, V. Venuti, P. Baglioni, E. Fratini, C. Vannucci, H.E. Stanley, The role of the solvent in the dynamical transitions of proteins: the case of the lysozyme–water system, *J. Chem. Phys.* 127 (2007) 045104.
- [145] F. Mallamace, C. Branca, M. Broccio, C. Corsaro, C.Y. Mou, S.H. Chen, The anomalous behavior of the density of water in the range $30\text{ K} < T < 373\text{ K}$, *Proc. Natl. Acad. Sci. USA* 104 (2007) 18387–18392.
- [146] C. Corsaro, J. Spooren, C. Branca, N. Leone, M. Broccio, C. Kim, S.-H. Chen, H.E. Stanley, F. Mallamace, Clustering dynamics in water/methanol mixtures: a nuclear magnetic resonance study at $205\text{ K} < T < 295\text{ K}$, *J. Phys. Chem. B* 112 (2008) 10449–10454.
- [147] F. Mallamace, C. Corsaro, M. Broccio, C. Branca, N. González-Segredo, J. Spooren, S.-H. Chen, H.E. Stanley, NMR evidence of a sharp change in a measure of local order in deeply supercooled confined water, *Proc. Natl. Acad. Sci. USA* 105 (2008) 12725–12729.
- [148] H.E. Stanley, S.V. Buldyrev, M. Canpolat, O. Mishima, M.R. Sadr-Lahijany, A. Scala, F.W. Starr, The puzzling behavior of water at very low temperature, *Phys. Chem. Chem. Phys.* (PCCP) 2 (2000) 1551–1558.
- [149] O. Mishima, H.E. Stanley, The relationship between liquid, supercooled and glassy water, *Nature* 396 (1998) 329–335.
- [150] C. Huang, K.T. Wikfeldt, T. Tokushima, D. Nordlund, Y. Harada, U. Bergmann, M. Niebuhr, T.M. Weiss, Y. Horikawa, M. Leetmaa, M.P. Ljungberg, O. Takahashi, A. Lenz, L. Ojamäe, A.P. Lyubartsev, S. Shin, L.G.M. Pettersson, A. Nilsson, The inhomogeneous structure of water at ambient conditions, *Proc. Natl. Acad. Sci. USA* 106 (2009) 15214–15218.
- [151] C. Huang, T.M. Weiss, D. Nordlund, K.T. Wikfeldt, L.G.M. Pettersson, A. Nilsson, Apparent Power Law Increase of Correlation Length in Bulk Supercooled Water, *J. Chem. Phys.* 133 (2010) 134504.
- [152] A. Geiger, H.E. Stanley, Low-density patches in the hydrogen-bonded network of liquid water: evidence from molecular dynamics computer simulations, *Phys. Rev. Lett.* 49 (1982) 1749–1752.
- [153] A. Geiger, H.E. Stanley, Tests of universality of percolation exponents for a 3-dimensional continuum system of interacting waterlike particles, *Phys. Rev. Lett.* 49 (1982) 1895–1898.